Production of Hydroxyl Radicals in the Dark

by:

Do Young Maeng

Contents

1. Abstract

Oxidation is prevalent in atmospheric chemistry due to the abundance of oxidants in the atmosphere. One of the commonly found oxidants is hydroxyl (OH) radical. Previously, OH radicals have been generated by means of UV photolysis, but the concurrent presence of photolysis and oxidation makes it challenging to pinpoint the exact mechanism behind the reactions occurring in the environmental chamber. Thus, a method for the production of OH radicals in a dark environment would be highly beneficial for decoupling the OH radical initiated-oxidation chemistry from photolysis. A method involving the ozonolysis of 2,3-dimethyl-2-butene (tetramethylethylene, TME) has been proposed by researchers from Center for Atmospheric Particle Studies in Carnegie Mellon University. We further investigated the feasibility of TME ozonolysis as a dependable source of OH radicals in a dark environment. Using the TME + O_3 method, we estimated the produced OH concentrations to be approximately 10^7~10^8 molecules cm^{-3}.

2. Introduction

Hydroxyl (OH) radicals are strong oxidizing agents naturally found in the troposphere. Due to their high reactivity, OH radicals partake in a multitude of important atmospheric chemistry processes including the formation of secondary organic aerosol (SOA)[1]. Atmoshperic chemistry and SOA formation are simulated and studied within an environmental chamber—a large temperature-controlled Teflon reactor shown below in Figure 1.

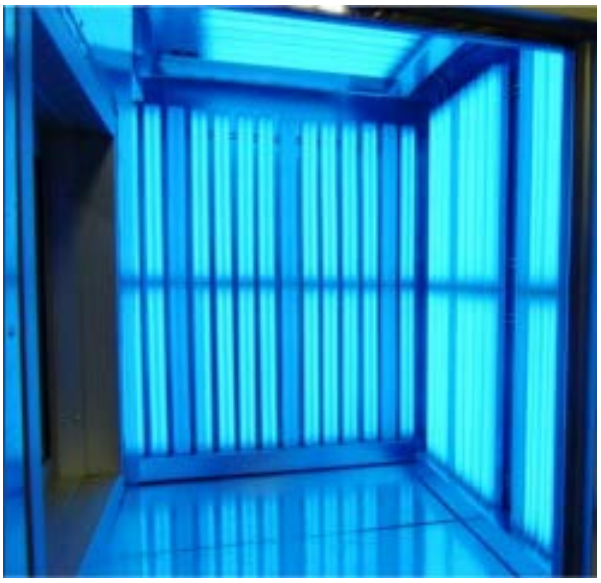

Figure 1. UT Austin environmental chamber enclosure—it houses the 10 m^3 Teflon reactor. Its walls have UV lamps installed for photochemical purposes such as photolysis.

Production of OH radicals has been accomplished via UV photolysis of nitrous acid (HONO) or hydrogen peroxide (H_2O_2). This method is simple and reliable; it produces an ample amount of OH radicals to attain typical concentration levels similar to that of the atmosphere (10^6 molecules cm^{-3}), and it does not require an intricate set-up. However, this method has both photolysis and oxidation occurring concurrently in the system; if another chemical species in the chamber is vulnerable to photolysis while the OH-initiated oxidation is occurring, then complications in determining the reaction mechanisms arise. A method to produce OH radicals without the presence of light is necessary to completely separate the effects produced by oxidation chemistry from the effects produced by photolysis.

3. Background

3.1 Reaction Mechanism

Several alkene-ozone reactions can function as an OH radical production pathway in a dark environment, but Lambe et al. selected 2,3-dimethyl-2-butene, commonly denoted as TME (C_6H_{12}), as their choice of alkene for various reasons[2]. Firstly, the efficiency of TME ozonolysis is near unity (100%)[3]. Secondly, the products of TME ozonolysis have high vapor pressures and therefore do not form organic aerosol[2].

Lambe et al. suggested the following three chemical reactions to mainly consider when designing the system:

$$\mathrm{TME} + \mathrm{O_3} \rightarrow \mathrm{OH} + \mathrm{products}$$
$$\mathrm{TME} + \mathrm{OH} \rightarrow \mathrm{products}$$
$$\mathrm{OH} + \mathrm{species\ of\ interest} \rightarrow \mathrm{products}$$

The Master Chemical Mechanism (MCM) provided further detail on the reaction pathways of TME[4]:

$$\mathrm{TME} + \mathrm{O_3} \rightarrow \mathrm{C_3H_6O_2} + \mathrm{C_3H_6O}$$
$$\mathrm{C_3H_6O_2} + \mathrm{O_2} \rightarrow \mathrm{C_3H_5O_3} + \mathrm{OH}$$
$$\mathrm{TME} + \mathrm{OH} \rightarrow \mathrm{C_6H_{13}O_3}$$

The products of the TME + ozone (O_3) reaction, $C_3H_6O_2$ and C_3H_6O, were particularly important in this study, as they acted as primary indicators as to whether or not the ozonolysis of TME was occurring in the chamber.

To ensure that the OH radicals are plentiful for the oxidation reaction of our species of interest, bringing the reaction of TME + OH to a negligible reaction rate was imperative. This issue could be resolved by maintaining a low concentration level of TME at all times via simultaneous injection of TME and O_3 and starting the system with a relatively high initial concentration of ozone[2]. However, to circumvent the complexities associated with the ozone generator, we decided to forgo the simultaneous injection and opted only for the high initial charge of ozone.

By performing mass balances of accumulation = input + generation – output – consumption, the changes in the concentrations of the reactants over time—disregarding the reaction of OH + species of interest—are as follows:

$$\frac{\partial C_{TME}}{\partial t} = \theta_{TME} - k_{O_3}^{TME} C_{TME} C_{O_3} - k_{OH}^{TME} C_{TME} C_{OH} \quad (1)$$
$$\frac{\partial C_{O_3}}{\partial t} = -k_{O_3}^{TME} C_{TME} C_{O_3} \quad (2)$$
$$\frac{\partial C_{OH}}{\partial t} = k_{O_3}^{TME} C_{TME} C_{O_3} - k_{OH}^{TME} C_{TME} C_{OH} \quad (3)$$

where C_x is the concentration of species x, k_y^x is the second-order rate constant of the reaction x + y, and θ_x is the particle flux of species x into the chamber.

Because the concentration of O_3 was at an extremely high level throughout the duration of the experiment, $k_{O_3}^{TME} C_{O_3} >> k_{OH}^{TME} C_{OH}$. The reaction rate of TME + OH was thus negligible, and we further simplified equations (1)-(3) into:

$$\frac{\partial C_{TME}}{\partial t} = \theta_{TME} - k_{O_3}^{TME} C_{TME} C_{O_3} \quad (4)$$
$$\frac{\partial C_{O_3}}{\partial t} = -k_{O_3}^{TME} C_{TME} C_{O_3} \quad (5)$$
$$\frac{\partial C_{OH}}{\partial t} = k_{O_3}^{TME} C_{TME} C_{O_3} \quad (6)$$

Ideally, the production of OH would be continuous and steady, consisting of a constant $\partial C_{OH}/\partial t$. For this to happen, $C_{TME}C_{O_3}$ must be constant which requires keeping concentrations of both TME and O_3 at a steady-state

level. To achieve such steady-state conditions for TME and O_3, we sustained a low flux of TME to retain the concentration level of TME while charging the system with an excessive amount of ozone.

3.2 TME Injection

Maintaining a low concentration level of TME is achievable if TME injection into the chamber is constrained to a low, steady flow rate, preventing the accumulation of TME in the chamber; Lambe et al. used capillary tubes to reach such low, steady flow rates in the range of 0.03 $mL \cdot hr^{-1}$ and 0.12 $mL \cdot hr^{-1}$.

With capillary's microscale flow channel, we could safely characterize the TME flow as laminar flow and used Poiseuille's Law to calculate the flow rate of TME:

$$Q = \frac{\pi(\Delta P)r^4}{8\eta l} \quad (7)$$

where ΔP is the pressure gradient, r is the inner radius of the channel, η is the viscosity of the fluid, and l is the length of the channel.

The viscosity of TME was calculated using the following equation:

$$log_{10}\,\eta_{liq} = A + \frac{B}{T} + (C \times T) + (D \times T^2) \quad (8)$$

where η_{liq} is the viscosity of TME in centipoise, T is temperature in Kelvin, and A, B, C, and D are constants with values of -12.0073, 1.5593E03, 2.9831E-02, and -2.9491E-05 respectively[5].

3.3 Tracer Species Selection

A tracer species was injected into the chamber to verify the production of OH radicals and to quantify the OH radicals produced. By injecting a predetermined amount of the tracer and tracking its consumption from its reaction with the OH radicals, measuring the concentration of OH radicals in the chamber was feasible. The most important criteria when selecting the tracer species was its reactivity preference between OH radicals and O_3. We would like to attribute the decrease in the concentration of tracer species to its reaction with OH radicals; therefore, choosing a tracer which reacts favorably and at a much faster rate with OH radicals than with O_3 was paramount for approximating the OH radical concentration. We selected toluene as the tracer species and tracked its decay over time, as its reaction rate with OH radicals was faster by several degrees of magnitude than its reaction rate with O_3. Section 4.5 provides further detail on the calculations involving tracer species selection process.

4. Simulations and Calculations

4.1 TME Controlled Injection

In order to determine the TME particle flux into the chamber, we first calculated the volumetric flow rate of TME through the capillary tube by applying the aforementioned Poiseuille's Law. The pressure and temperature of the injection system are adjustable, but the length and the inner diameter of the capillary tube are not. Hence, Figures 2 and 3 below have been plotted in MATLAB to determine the adequate length and inner diameter of the capillary tubing under easily attainable temperature and pressure conditions (i.e. room temperature and low pressure difference):

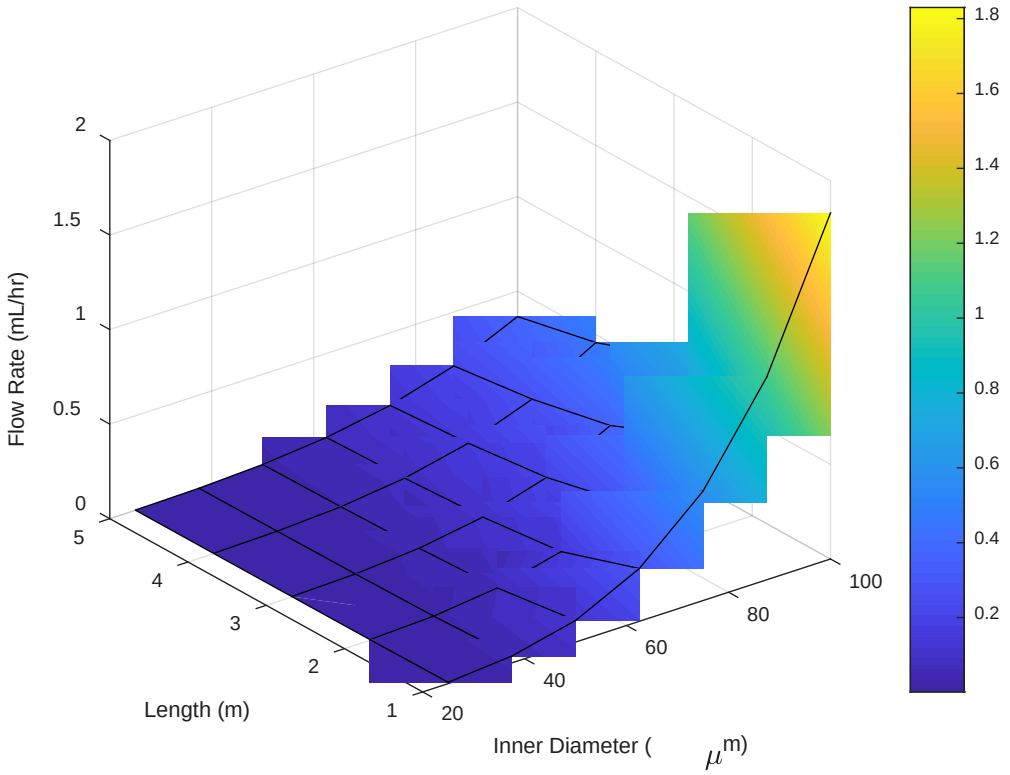

Figure 2. Flow rate of TME vs. capillary tube length and inner diameter at T = 293.15 K and dP = 10 psi.

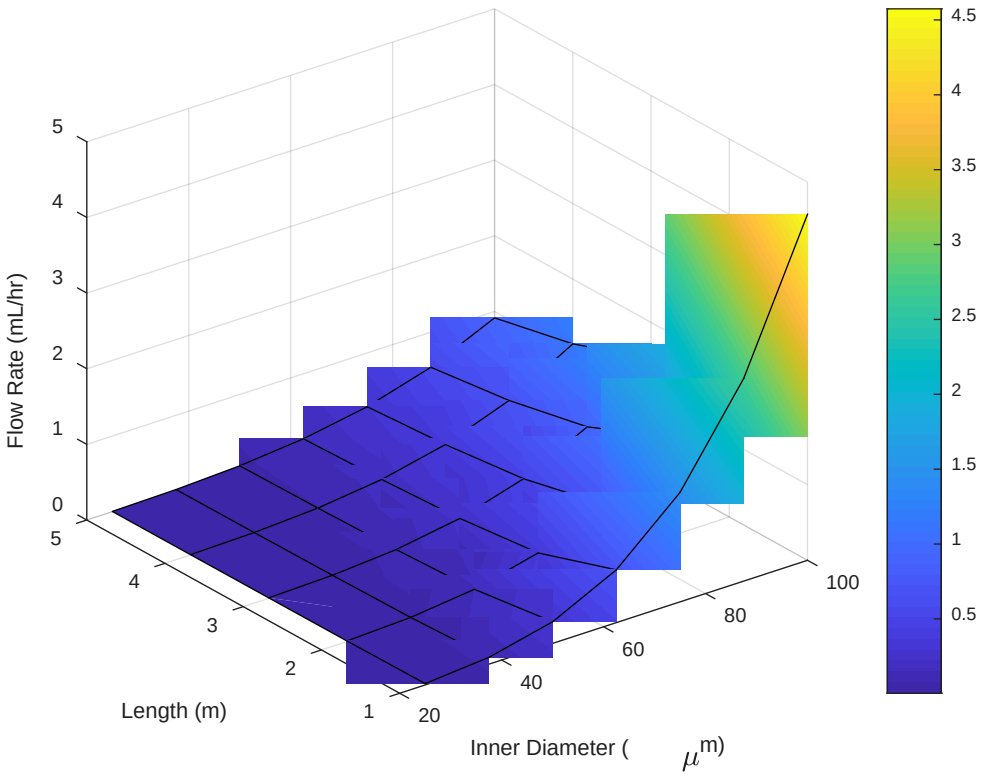

Figure 3. Flow rate of TME vs. capillary tube length and inner diameter at T = 293.15 K and dP = 25 psi.

Figures 2 and 3 indicate that the longer and narrower capillary tubes perform the best for our purposes of restricting the TME flow rate to values of 10^{-2}~10^{-1} mL·hr^{-1}. We chose Polymicro Technologies' fused silica capillary tubing (model TSP075375, I.D. 75 ± 3 μm, length 3 m). The linear correlation between flow rate and pressure difference—the most accessible controlled variable—is shown in Figure 4 below.

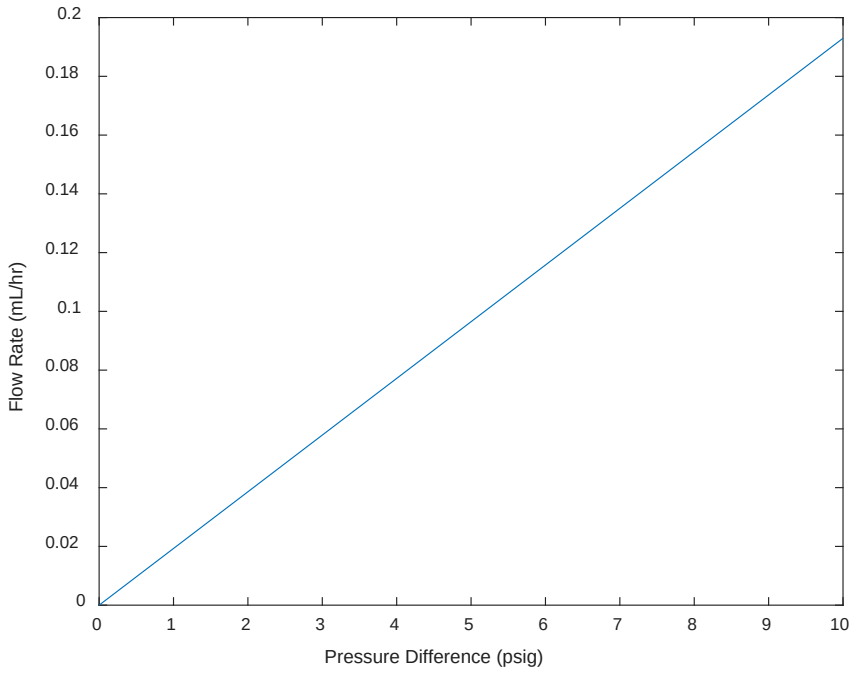

Figure 4. Volumetric Flow Rate of TME vs. Pressure Difference.

At T = 293.15 K and dP = 5 psig, TME would have a viscosity of 4.8294E-08 psi·s, and its volumetric flow rate through the capillary tube would be:

$$Q_{TME} = \frac{\pi \times 5\ psi \times (37.5 \times 10^{-6}\ m)^4}{8 \times (4.83 \times 10^{-8}\ psi \cdot s) \times 3\ m} \times \frac{10^6\ mL}{1\ m^3} \times \frac{3600\ s}{1\ hr} = 0.0965\ mL \cdot hr^{-1}$$

, which can be further converted into molar flow rate and particle flux into the 10 m^3 environmental chamber using density of TME at normal temperature condition and molecular weight[7]:

$$\dot{n}_{TME} = \frac{0.0965\ mL}{hr} * \frac{0.7188\ g}{mL} * \frac{1\ mol}{84.16\ g} = 8.2403 \times 10^{-4}\ mol \cdot hr^{-1}$$

$$\theta_{TME} = \frac{\dot{n}_{TME} \times N_A}{V_{chamber}}$$

$$\theta_{TME} = \frac{\frac{8.2403 \times 10^{-4}\ mol}{hr} \times \frac{6.022 \times 10^{23} molecules}{1\ mol} \times \frac{1\ hr}{3600\ s}}{10\ m^3 \times \frac{10^6\ cm^3}{1\ m^3}}$$

$$\theta_{TME} = 1.3784 \times 10^{10}\ molec \cdot cm^{-3} \cdot s^{-1}$$

With the volumetric flow rate calculated, the estimated time for TME to travel across the capillary tube was:

$$t_{TME-travel} = \frac{L_{tube}}{v}$$

$$t_{TME-travel} = \frac{L_{tube}}{\frac{Q_{TME}}{A_{tube}}}$$

$$t_{TME-travel} = \frac{300\ cm}{\frac{0.09629\ cm^3 \cdot hr^{-1}}{\pi \cdot (0.00375\ cm)^2}} = 0.138\ hr = 8.26\ min$$

, indicating that the production of OH radicals would occur approximately 8 minutes after the capillary injection has been pressurized.

4.2 Ozone Injection: Initial Concentration Preparation

Assuming accumulation of TME is negligible, initial ozone concentration must be several orders of magnitude higher than the TME particle flux to encourage the reaction of TME + O_3. Ozone concentrations of 10^{12}~10^{13} molecules·cm^{-3} were considered sufficient enough for $k_{O_3}^{TME} C_{O_3} >> k_{OH}^{TME} C_{OH}$ while maintaining OH radical concentration near the atmospheric level of 10^6 molecules·cm^{-3}.

The following series of calculations converts the initial O_3 concentration of 10^{13} molecules·cm^{-3} to mixing ratio in the chamber:

$$N_{O_3,chamber} = C_{O_3} \times V_{chamber}$$

$$N_{O_3,chamber} = \frac{10^{13}\ molecules}{cm^3} \times \left(10\ m^3 \times \frac{10^6\ cm^3}{1\ m^3}\right)$$

$$N_{O_3,chamber} = 10^{20}\ molecules$$

$$n_{O_3,chamber} = 1.66 \times 10^{-4} mol$$

$$N_{air,chamber} = \frac{V_{chamber} \times \rho_{air} \times N_A}{MW_{air}}$$

$$N_{air,chamber} = \frac{10\ m^3 \times \left(\frac{1.205\ kg}{m^3} \times \frac{1000\ g}{1\ kg}\right) \times \frac{6.022 \times 10^{23}\ molecules}{1\ mol}}{\frac{29\ g}{mol}}$$

$$N_{air,chamber} = 2.502 \times 10^{26}\ molecules$$

$$C_{O_3} = \left(\frac{N_{O_3,chamber}}{N_{O_3,chamber} + N_{air,chamber}} \times 10^9\right) ppb$$

$$C_{O_3} = \left(\frac{10^{20} molecules}{10^{20} molecules + 2.502 \times 10^{26} molecules} \times 10^9\right) ppb$$

$$C_{O_3} = 399.6\ ppb$$

Considering that the ozone generator TG-10 is able to provide approximately 1.9717E-5 mol·min^{-1} at output level 2 with 1 L·min^{-1} of oxygen input flow, we calculated the injection time to be:

$$t_{injection} = \frac{1.66 \times 10^{-4} mol}{\frac{3.4525 \times 10^{-4} mol}{min}} = 0.481\ min = 28.8\ s$$

4.3 Concentration Profile Modeling, Continuous Injection

Prior to the experiments, we modeled the reaction kinetics discussed in Equations 1-3 to quantify the production of OH radicals in the chamber over time. The reaction rate constants were found in Master Chemical mechanism website[4]:

$$k_{O_3}^{TME} = 3.03 \times 10^{-15} \times e^{\frac{-294}{Temp(K)}}\ cm^3 \cdot molec^{-1} \cdot s^{-1}$$
$$k_{OH}^{TME} = 1.10 \times 10^{-10}\ cm^3 \cdot molec^{-1} \cdot s^{-1}$$

The model simulated OH radical production under the parameters listed below:

$$C_{TME} = 0\ molec \cdot cm^{-3}$$
$$C_{O_3} = 10^{13}\ molec \cdot cm^{-3}$$
$$C_{OH} = 0\ molec \cdot cm^{-3}$$
$$\theta_{TME} = 1.3784 \times 10^{10}\ molec \cdot cm^{-3} \cdot s^{-1}$$

Continuous injection of TME and a high initial charge of ozone result in unsustainable levels of OH concentration as observed in the concentration profile below:

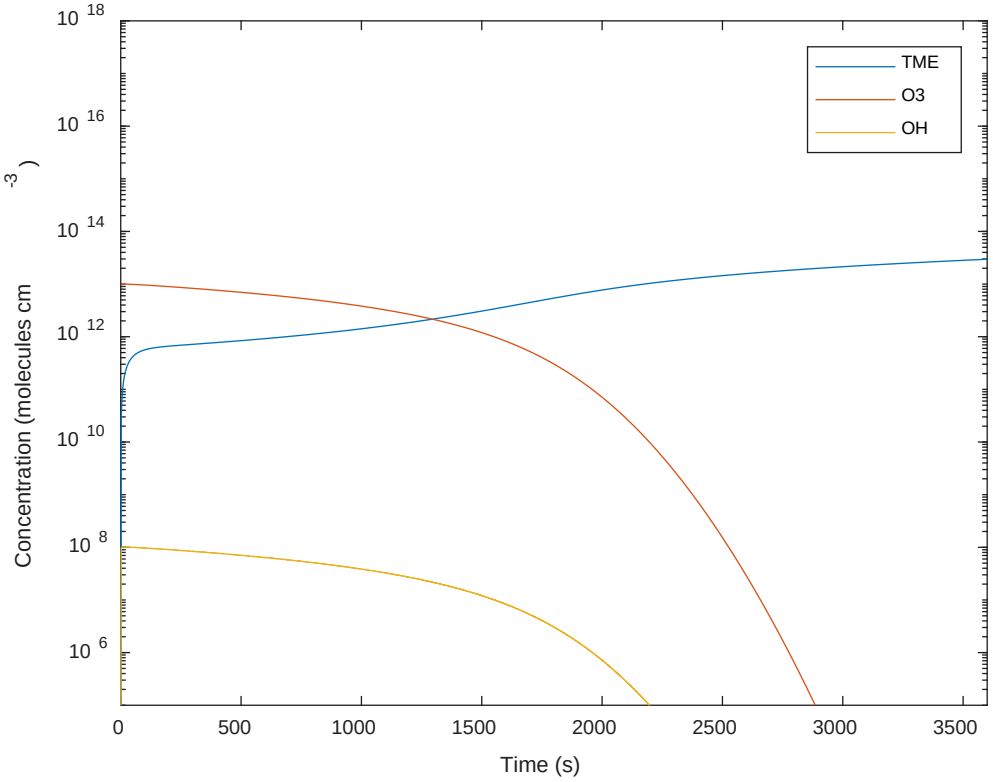

Figure 4. Concentrations of TME, O_3, and OH radicals as a function of time when TME is injected continuously.

Continuously injecting TME with no presence of continuous O_3 supply results in sharp depletion of O_3 near t = 1400 s when TME concentration surpasses that of O_3. This unsteady behavior in OH concentration is observed because the rate at which OH is consumed is faster than the rate at which it is generated; the reaction rate of TME + O_3 continuously diminishes over time while TME + OH reaction rate progressively increases. Ultimately, continuously injecting TME is not a viable method.

4.4 Concentration Profile Modeling, Non-Continuous Injection

Figures 5 and 6 show the concentration profiles of the three species plotted under same aforementioned parameters in Section 4.3 with injection periods limited to 10 and 20 minutes respectively.

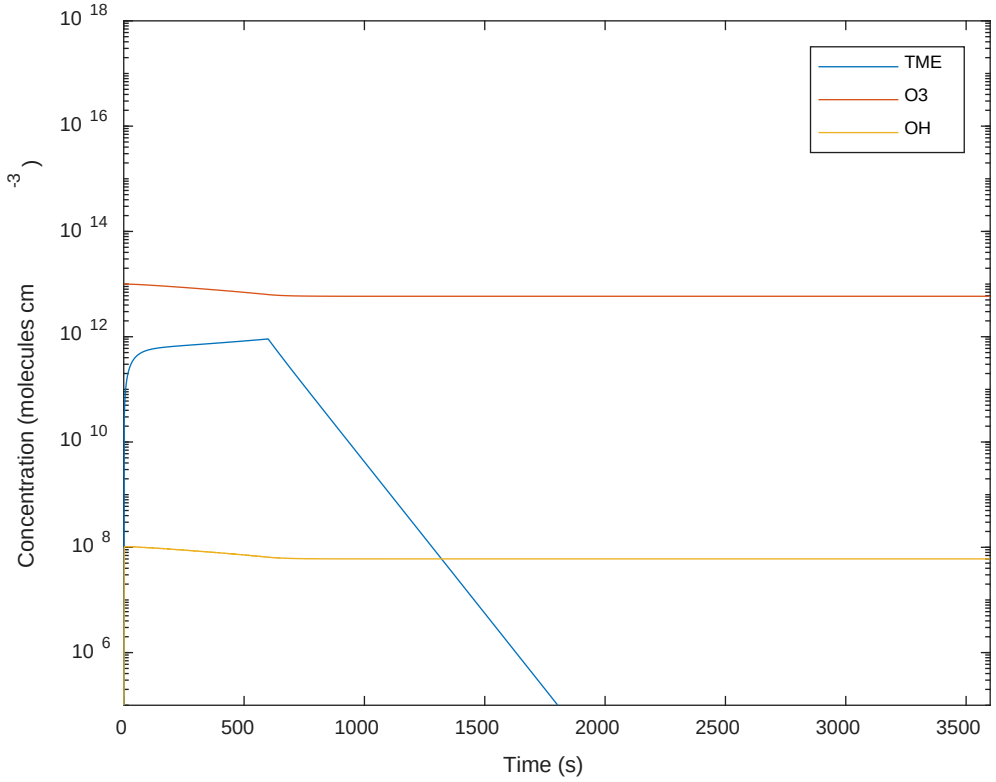

Figure 5. Concentrations of TME, O_3, and OH radicals as a function of time when TME is injected for the first 10 minutes.

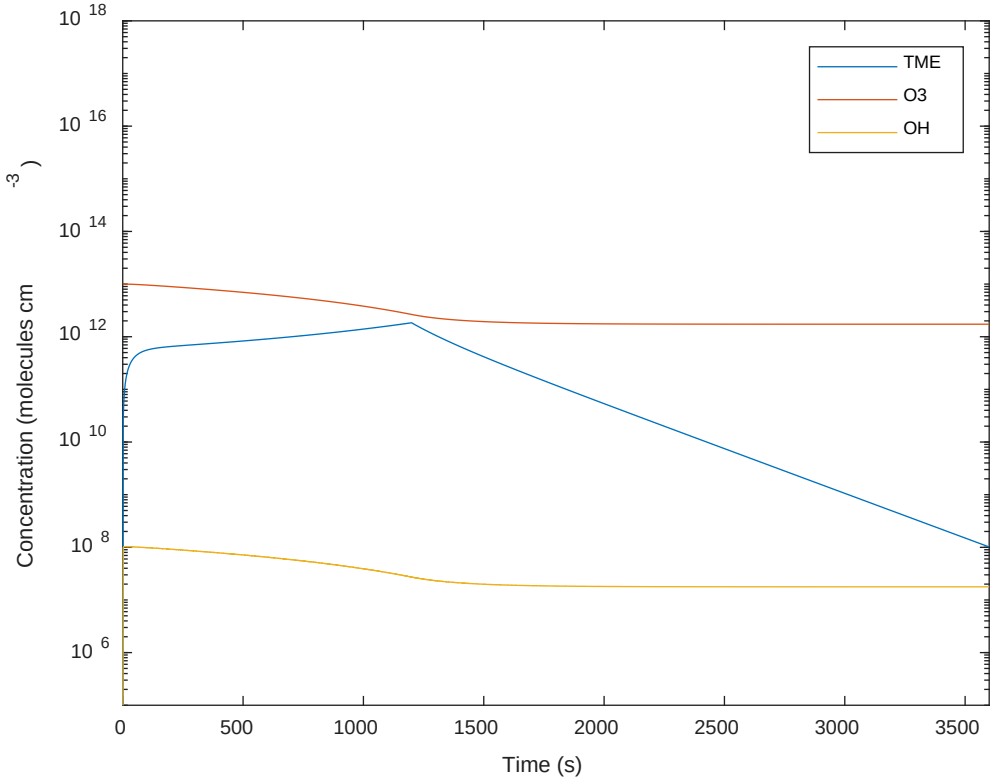

Figure 6. Concentrations of TME, O_3, and OH radicals as a function of time when TME is injected for the first 20 minutes.

In Figure 5 and 6, TME concentration declined steadily once the injection was halted. Ozone and OH radical concentrations remained stable once the injection was halted. A possible explanation for this pattern is the dynamic equilibrium of the system. As OH is consumed from its reaction with TME, TME reacts with ozone to further produce OH radicals, causing rapid depletion of TME while preserving OH radical concentration at a steady level. The concentration of ozone continuously decreases as well, but the rate at which it is consumed is much lower than the rate at which TME is consumed.

4.5 Tracer Reaction Rate

In order to check a chemical species' viability as a tracer, we compared the reaction rate of tracer + OH against the reaction rate of tracer + O_3 to ensure that the tracer would be consumed predominantly by OH radicals. Our target difference between the reaction rates was approximately one to two orders of magnitude. Assuming OH and O_3 concentrations to be 10^8 and 10^{13} molecules·cm^{-3}, we checked toluene's viability[8,9]:

$$k_{OH}^{C_7H_8} = 1.8 \times 10^{-12} \times e^{\frac{340}{Temp\ (K)}} = 5.741 \times 10^{-12}\ cm^3 \cdot molec^{-1} \cdot s^{-1}\ at\ T = 293.15\ K$$
$$k_{O_3}^{C_7H_8} = 1.2 \times 10^{-20}\ cm^3 \cdot molec^{-1} \cdot s^{-1}$$

$$r_{OH}^{C_7H_8} = k_{OH}^{C_7H_8} C_{C_7H_8} C_{OH} \approx k_{OH}^{C_7H_8} C_{OH}$$
$$r_{OH}^{C_7H_8} = (5.741 \times 10^{-12}\ cm^3 \cdot molec^{-1} \cdot s^{-1}) \times (10^8\ molec \cdot cm^{-3})$$
$$r_{OH}^{C_7H_8} = 5.741\ \times 10^{-4}\ s^{-1}$$

$$r_{O_3}^{C_7H_8} = k_{O_3}^{C_7H_8} C_{C_7H_8} C_{O_3}$$
$$r_{O_3}^{C_7H_8} = (1.2 \times 10^{-20}\ cm^3 \cdot molec^{-1} \cdot s^{-1}) \times (10^{13}\ molec \cdot cm^{-3})$$
$$r_{O_3}^{C_7H_8} = 1.2\ \times 10^{-7}\ s^{-1}$$

Because the reaction rate of toluene + O_3 is greater than toluene + ozone by three orders of magnitude, toluene would certainly be suitable as a tracer species.

4.6 OH Radical Concentration

Using the High Resolution Time-of-Flight Chemical Ionization Mass Spectrometer (HR ToF CIMS), we tracked the decay of toluene from its reactions with O_3 and OH to quantify the concentration of OH in the chamber:

$$-\frac{dC_{C_7H_8}}{dt} = k_{OH}^{C_7H_8} C_{C_7H_8} C_{OH} + k_{O_3}^{C_7H_8} C_{C_7H_8} C_{O_3}$$
$$ln(C_{C_7H_8}) = -(k_{OH}^{C_7H_8} C_{OH} + k_{O_3}^{C_7H_8} C_{O_3}) \cdot t + \mathrm{C}$$
$$C_{C_7H_8} = C_{C_7H_8,0} \cdot exp[-(k_{OH}^{C_7H_8} C_{OH} + k_{O_3}^{C_7H_8} C_{O_3}) \cdot t]$$

Note that at $t = \tau$, $C_{tol}/C_{tol,o} = e^{-1}$, which means

$$-1 = -(k_{OH}^{C_7H_8} C_{OH} + k_{O_3}^{C_7H_8} C_{O_3}) \cdot \tau$$
$$\tau = \frac{1}{k_{OH}^{C_7H_8} C_{OH} + k_{O_3}^{C_7H_8} C_{O_3}}$$

where τ is the lifetime of toluene obtained by fitting the decay to an exponential curve.

$$1697.6\ \mathrm{s} = \frac{1}{(5.741 \times 10^{-12}\ cm^3 \cdot molec^{-1} \cdot s^{-1}) C_{OH} + (1.2 \times 10^{-20}\ cm^3 \cdot molec^{-1} \cdot s^{-1})(1.9 \times 10^{13}\ molec \cdot cm^{-3})}$$

$C_{OH} = 1.025 \times 10^8\ molec \cdot cm^{-3}$

5. Experimental Methods

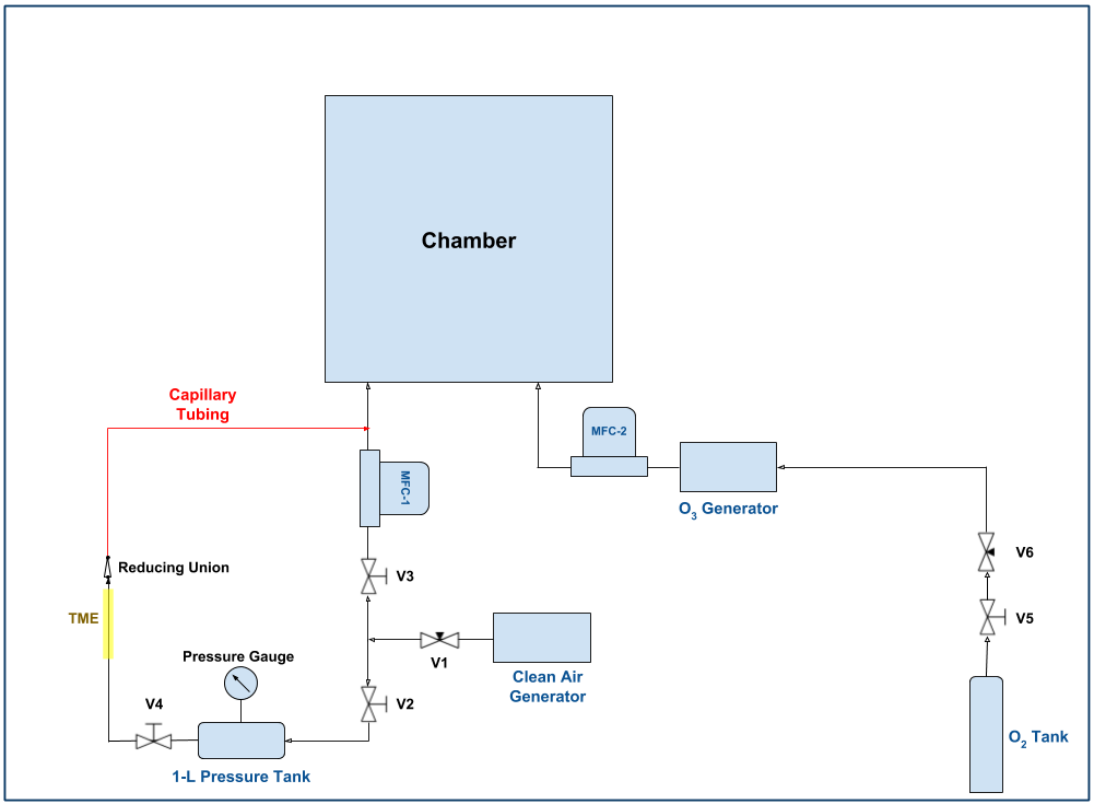

Figure 7. Schematic diagram of the dark OH radical generation system.

Figure 7 above illustrates the schematic diagram of the dark OH radical generation system. The TME inlet on the left side and the ozone inlet on the right side are connected to the 10 m^3 Teflon bag. The chamber was cleaned before and after each experiment by first injecting high amounts of ammonium sulfate and chlorine and then flushing the chamber with clean, dry air.

For the injection of O_3, valves 5 and 6 were opened to start the oxygen flow into the generator. The mass flow controller was placed downstream from the generator and set to 1 $L \cdot min^{-1}$. The ozone generator was turned on only for the specified time duration and was turned off for the remainder of the experiment.

For the injection of TME, only valves 1 and 2 were opened initially to pressurize the tank with clean air. Valve 2 was closed once the gauge indicated a desirable level of pressure in the tank. The TME reservoir, a 10 cm Teflon tube connected vertically to the tank's nozzle, was filled with 0.2-0.3 mL of TME; TME was added in excess to assure that the entry point to the capillary tube was completely submerged in TME and to offset possible losses from leaks or vaporization of the chemical. Once the tank and the TME reservoir were charged, valve 3 was opened in order to induce flow across the capillary tube, and valve 4 was also opened to operate the carrier flow transferring the TME into the chamber.

The dark OH radical generation system was tested three times in order to gauge its stability and reproducibility. The order of injection for all three experiments was toluene, O_3, and TME. An undisturbed decay pattern in toluene signals was essential in accurately quantifying the concentration of OH radicals, so toluene was introduced first, providing enough time for the chamber to be well-mixed and thus obtaining a more stable toluene signal from CIMS prior to initiating any chemical reactions.

Table 1. Experiment Parameters

Experiment #	Initial CO3		dP, Pressure Tank (psig)	Predicted TME Input Flow Rate (mL/hr)	Predicted TME Input Flux (10^{10} molec cm-3 s-1)	Approximate TME Injection Duration (min)
	(ppb)	(10^{12} molec cm^{-3})				
1	1100	27.5	15	0.289	4.14	40
2	78	1.95	10	0.193	2.76	40
3	760	19.0	5	0.0965	1.38	30

Table 1 above summarizes the experimental parameters for the three OH generation experiments. The amount of initial O_3 concentration varied for each experiment due to the O_3 generator malfunction. However, the differences in O_3 concentration likely did not affect the production of OH radicals as the depletion of OH radicals were mostly determined by the amount of TME in the chamber. To examine the relationship between TME input and the production of OH radicals, TME input flow rate was reduced across the experiments by reducing the pressure in the tank.

Approximate TME injection duration refers to the period during which TME injection system was activated. It was set to 30~40 minutes under the assumption that TME takes approximately 10 minutes to travel across the capillary tube. This likely resulted in a real TME injection duration—period during which TME is truly entering the chamber—of 20~30 minutes. The TME injection duration is discussed in greater detail in Section 6.1.

In the analysis of CIMS signal data, products of TME + O3 and toluene + OH were used as indicators in confirming the production of OH radicals. Chemical species of interest and their mass-to-charge are tabulated in Table 2 below. After normalizing all measurements with the H_5O_2+ signal as the reference, changes in the signal of $C_3H_7O^+$ (the protonated form of a TME ozonolysis product) were observed to detect the production of OH radicals in the chamber, and changes in the signal of $C_7H_9^+$ (protonated toluene) were observed to quantify the concentration of OH radicals. The lifetime of toluene was obtained by analyzing the CIMS data with Tofware and fitting the treated $C_7H_9^+$ signal to an exponential decay curve. The OH radical concentration was calculated after obtaining the lifetime of toluene as previously shown in Section 4.6.

Table 2. Chemical Species of Interest

Common Name	Chemical Formula	Molecular Weight	Chemical Formula, Ionized	Mass-to-Charge Ratio	Notes
Water (Hydronium)	H2O	18.015	H3O+	19.02	N/A
Water hydrate	H4O2	36.03	H5O2+	37.04	N/A
Water dihydrate	H6O3	54.045	H7O3+	55.0538	N/A
N/A	C3H6O	58.0791	C3H7O+	59.0871	Product of TME Ozonolysis
N/A	C3H6O2	74.0785	C3H7O2+	75.0865	Product of TME Ozonolysis
N/A	C5H8O2	100.1158	C5H9O2+	101.1243	Product of TME Ozonolysis (Presumably)
Toluene	C7H8	92.1384	C7H9+	93.1464	N/A
N/A	C5H6O2	98.0999	C5H7O2+	99.1084	Product of Tolune + OH

6. Result and Discussion

6.1 TME Injection Duration

Figures 8 through 10 below show the changes in $C_3H_7O^+$ (m/z = 59) signal over time in Experiments 1 through 3 respectively. While there were significant increases in $C_3H_7O^+$ signal following the injection of TME in all of the experiments, the signals fluctuated too heavily at random or at injection of ozone into the chamber. Consequently, the signals were not stable enough to pinpoint the exact time at which TME is introduced into the chamber. This instability was observed in signals of other product species mentioned in the Methods section unfortunately, so it is currently not possible to precisely time the period during which TME was entering the chamber.

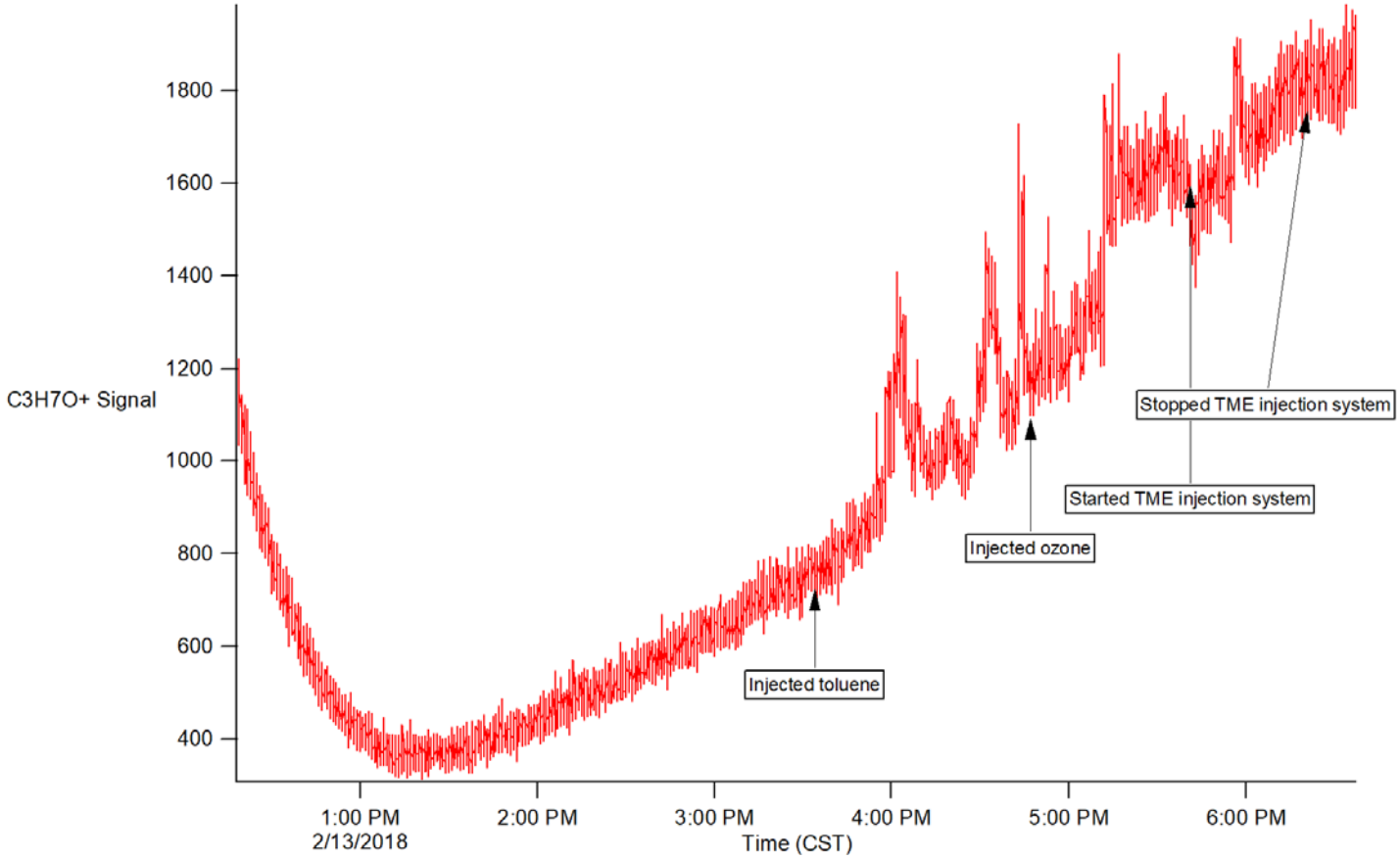

Figure 8. Experiment 1, observed $C_3H_7O^+$ ion signal over time.

In Experiment 1, the signal of $C_3H_7O^+$ ion was extremely unstable at the start of the experiment; it gradually decreased to low levels around 1:20 PM but steadily increased afterwards despite the absence of any organic injection. A possible explanation of such behavior is the presence of organic residues in the chamber prior to the experiment, but the cause of this behavior is currently uncertain. A spike in signal is present when ozone is injected, but the signal also increases significantly between O_3 injection and TME injection. This increase suggests that the TME injection system had been functioning before it was activated, possibly because the outlet end of the tubing was not perfectly at atmospheric pressure.

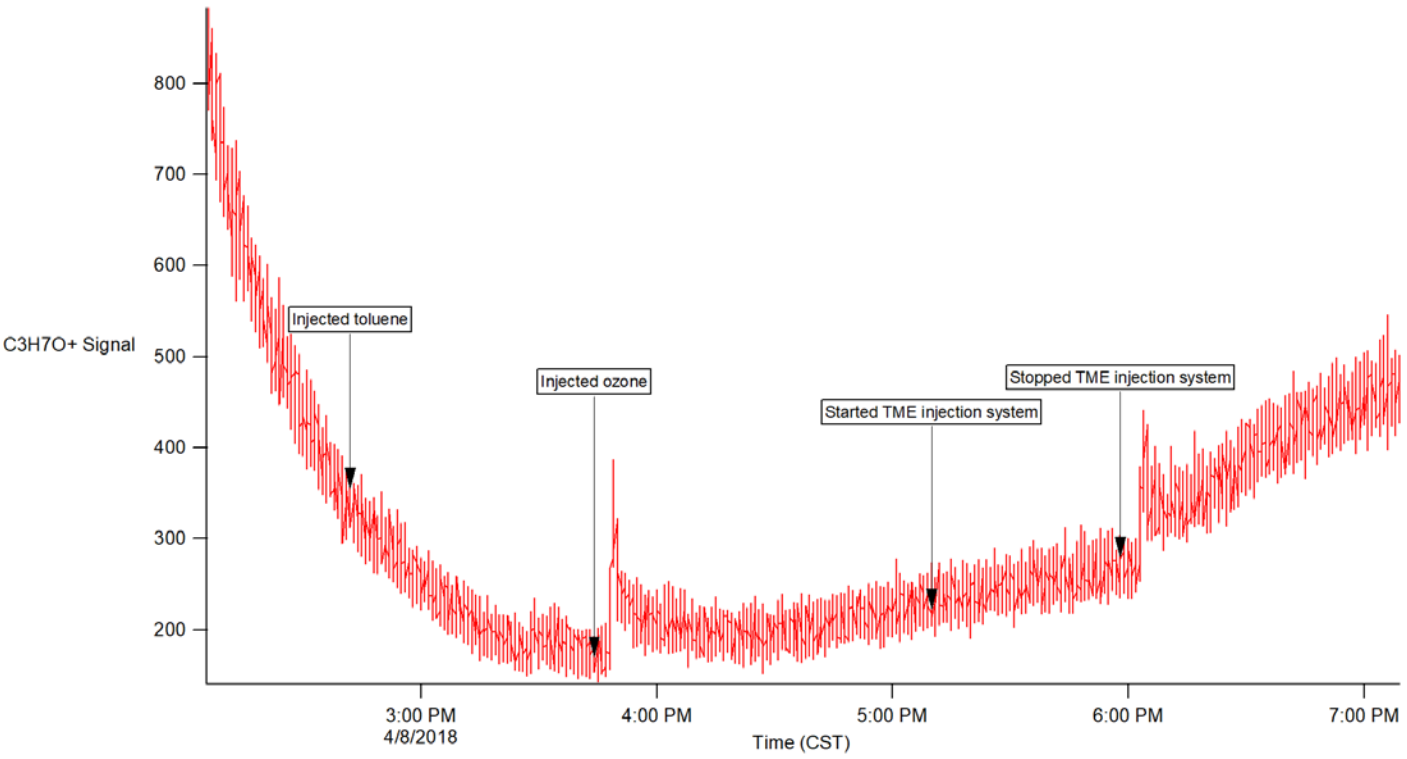

Figure 9. Experiment 2, observed $C_3H_7O^+$ ion signal over time.

In Experiment 2, the signal shows an initial decay trend and a spike during ozone injection similar to the Experiment 1 observations. The signal increases in intensity between O3 injection and TME injection but at a much lower rate than it had in Experiment 2. The signal spikes once more after the TME injection was completed. Considering there is a steady clean air flow into the chamber during the injection, the instability in the detection of $C_3H_7O^+$ may arise from this clean air flow disturbance in the reactor.

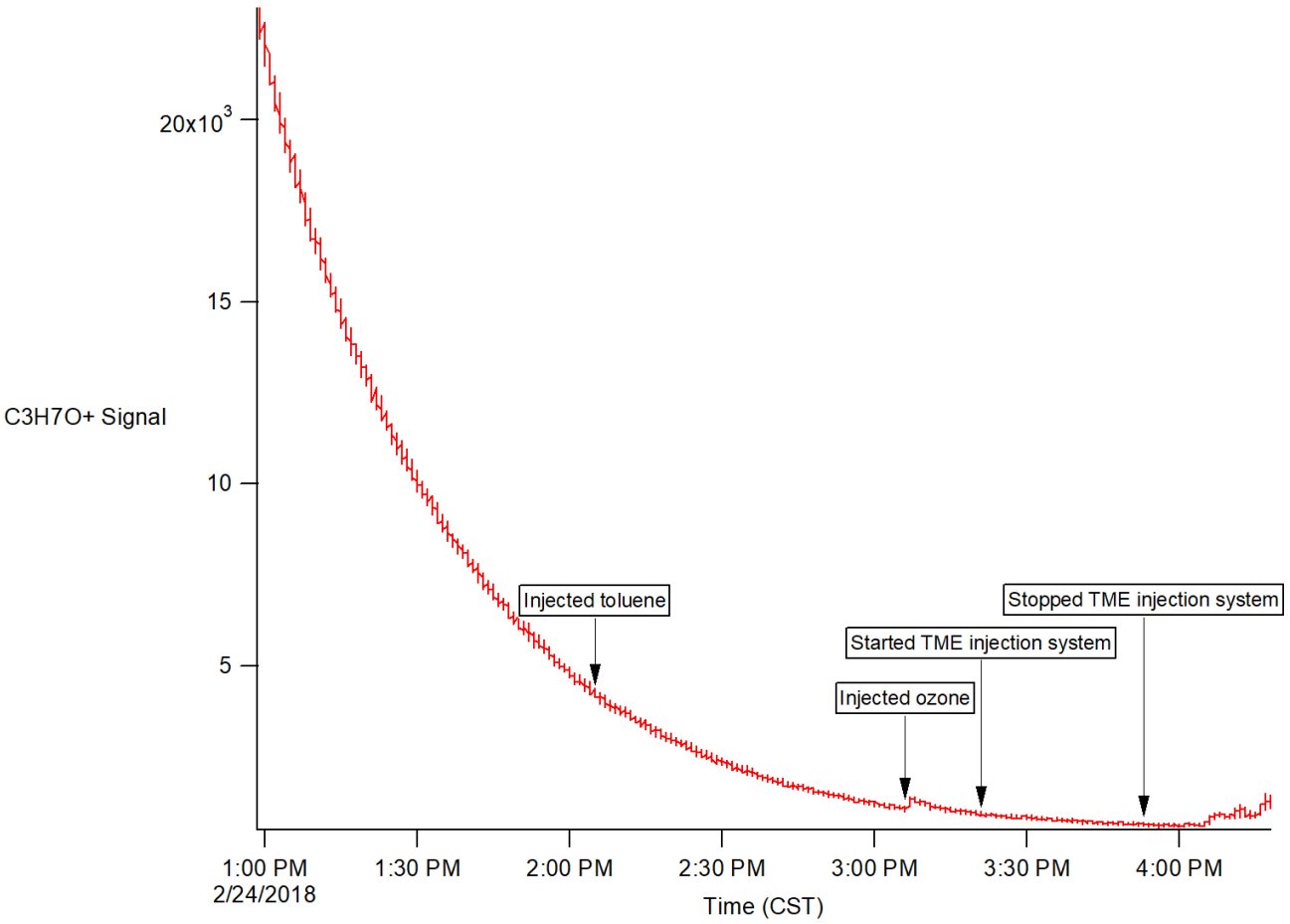

Figure 10. Experiment 3, observed $C_3H_7O^+$ ion signal over time.

In Experiment 3, the signal is at a much higher intensity of 20000 when compared to the values of 800~1200 in Experiments 1 and 2. Aside from the small spike at ozone injection, the signal showed a trend of exponential decay and, similarly to Experiment 2 observations, increased once TME injection was complete. As mentioned earlier in this section, this delay may arise from the carrier air flow's disturbance in the reactor. Further investigation is recommended to ascertain the cause of this delay in $C_3H_7O^+$ signal.

6.2 Observed Toluene Decay and Concentration of OH Radicals

The changes in toluene ion signal over time for Experiments 1 through 3 are shown in Figures 11 through 13 respectively. The signal data were fit to exponential decay only past the point at which the TME injection has stopped, as the precise time at which OH radical production starts is unclear. Similar to $C_3H_7O^+$ ion signals, toluene ion signals also spiked when ozone was injected into the chamber. We successfully fit the toluene signal curve to an exponential decay for experiments 2 and 3, but the toluene signal curve in Experiment 1 oscillated too heavily and could not be fit. Considering that the TME input was the highest in experiment 1, it is likely that the OH radicals were consumed by the excessive amount of TME, only present in negligible amounts in the chamber.

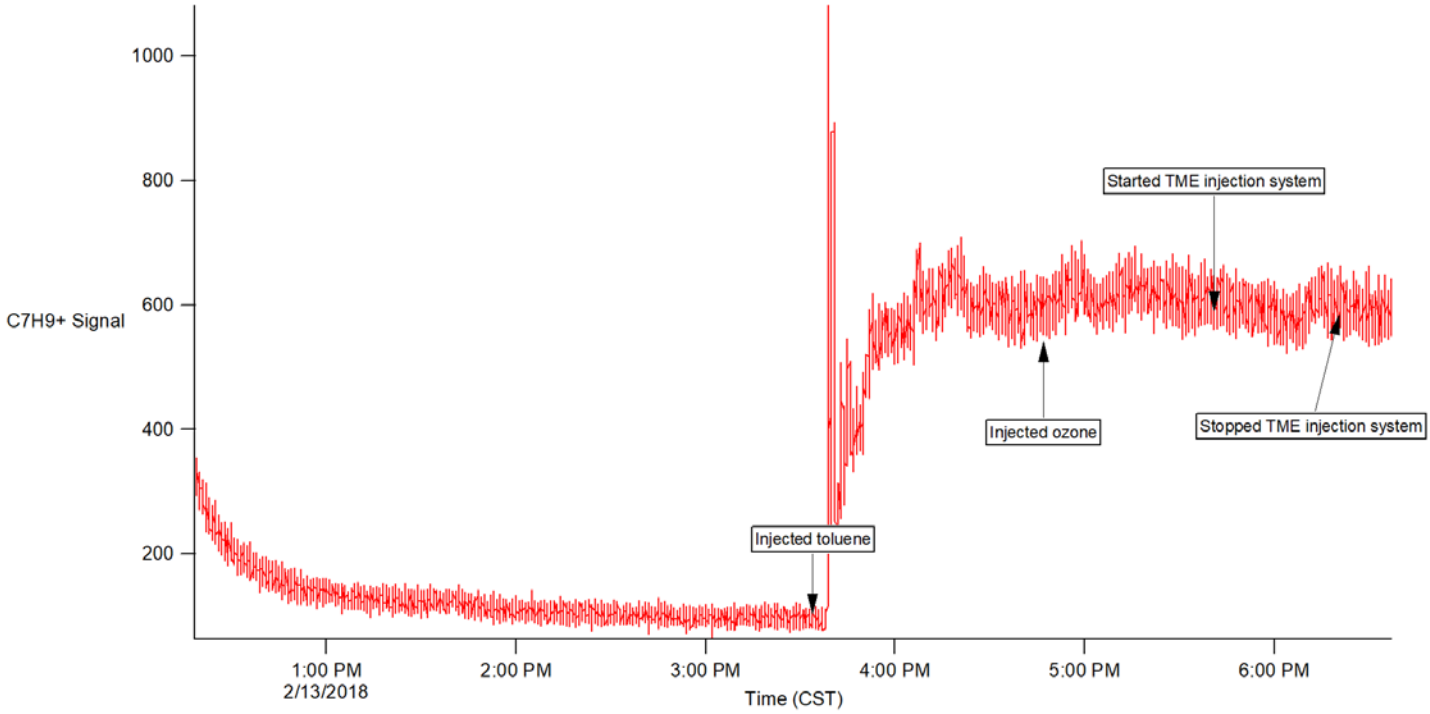

Figure 11. Experiment 1, observed toluene decay over time.

The toluene signal in Experiment 1 was noticeably unstable compared to the other two experiments. The instability in both toluene and $C_3H_7O^+$ signals suggest that the results observed from Experiment 1 are erroneous, presumably from instrument misconfiguration, faulty inlets/outlets, or the presence of residues before the start of the experiment.

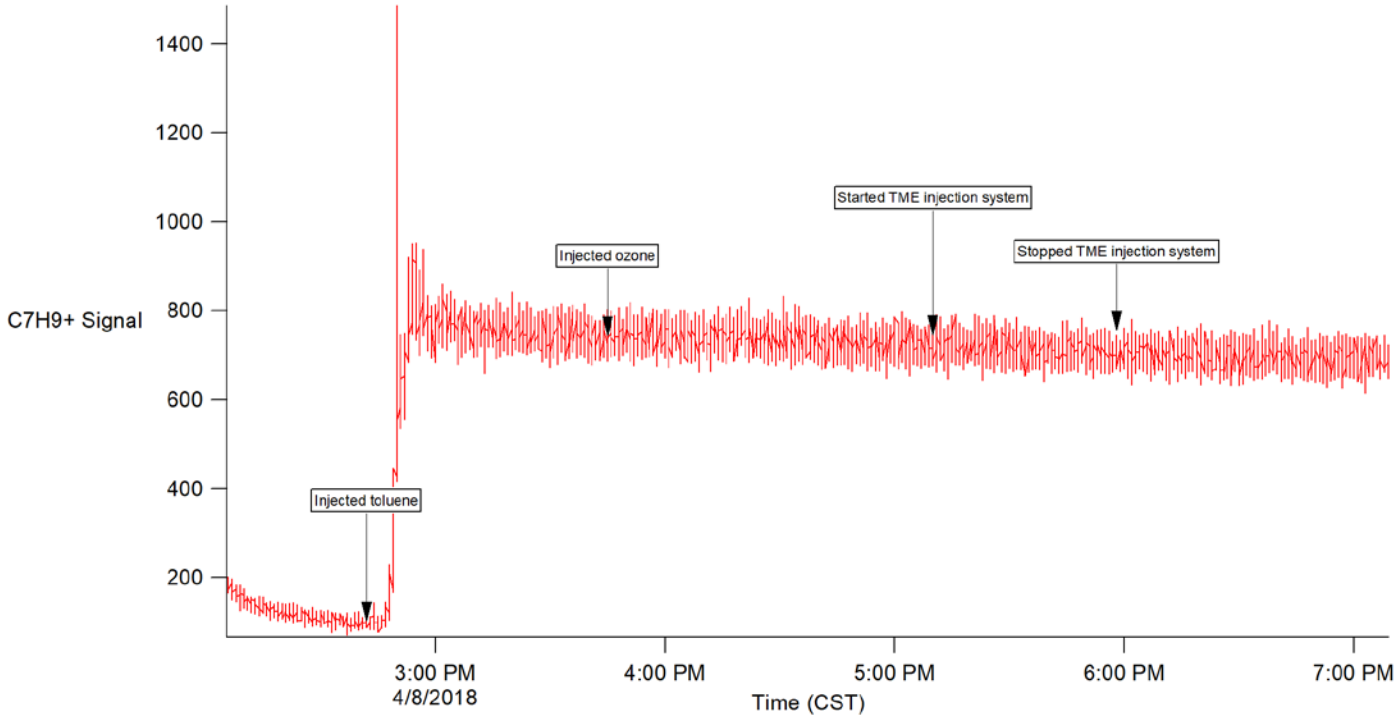

Figure 12. Experiment 2, observed toluene decay over time.

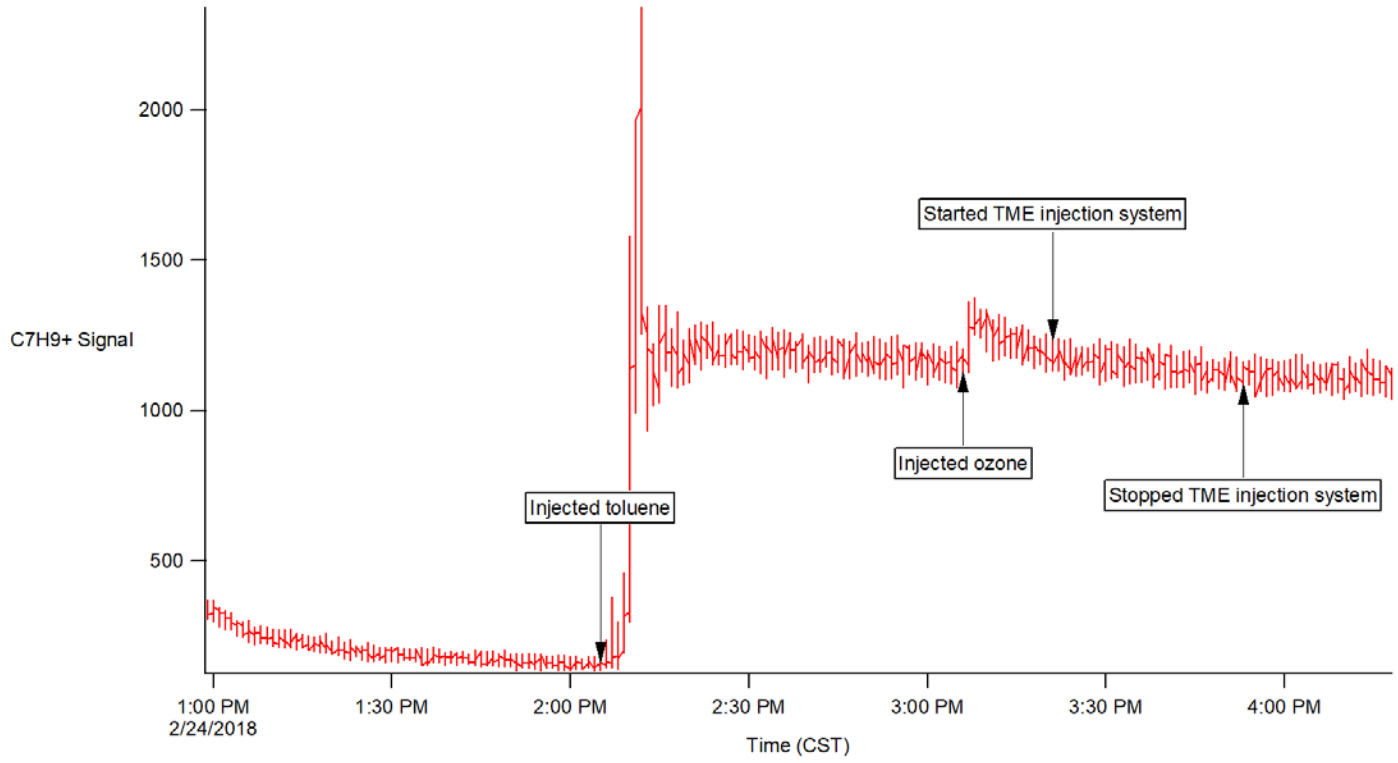

Figure 13. Experiment 3, observed toluene decay over time.

Figures 12 and 13 above show the toluene signal in Experiments 2 and 3 respectively. While the effect of TME is not noticeable with the naked eye, the lifetime values of toluene before and after the TME injection were significantly different.

Fitting the section of the curve prior to TME injection in Experiment 2 to an exponential decay resulted in toluene lifetime of 40000 s. However, performing a similar fit to the curve in Experiment 3 resulted in toluene lifetime of 500 s; the significant difference between the two lifetime values indicate that the experiments must be further repeated to determine which of these values was an outlier.

The lifetime values obtained when fitting the section of the curve after the TME injection for the two experiments were relatively precise, resulting in values of 1697.6 s and 2295.3 s for Experiments 2 and 3 respectively. The obtained lifetime and calculated OH radical concentration values are tabulated in Table 3 below.

Table 3. Toluene Lifetime and Observed OH Concentration

Experiment #	Toluene Lifetime (s)	Observed C_{OH} (molec cm^{-3})
1	N/A	N/A
2	2295.3	7.589×10^{7}
3	1697.6	1.025×10^{8}

The predicted concentrations of OH radicals for experiments 2 and 3 were 7.589E07 and 1.025E08 molecules·cm^{-3}, which closely matched the model's predicted value in Section 4.4. The difference in OH concentration values between the two experiments could be attributed to the increase in TME input, as increasing the TME input over a certain threshold results in significant OH radical loss. The current system provides the chamber with a single charge of OH radicals instead of a constant supply, so exceeding the atmospheric levels of 10^{6} molecules·cm^{-3} would be necessary in most circumstances to replicate the atmospheric conditions in the chamber.

The dark OH radical production system must be further tested in order to gauge its reliability. While the three experiments performed show a lot of promise, a lot of uncertainties remain on the TME injection duration and the signal stability of TME + O_3 products.

7. Acknowledgements

Thank you to Dr. Hildebrandt Ruiz and her graduate research assistants Surya Venkatesh, Sahil Bhandari, and Simon Wang for mentoring me and providing me the opportunity to work on this independent study. Funding for this project was provided in part by the State of Texas as part of the program of the Texas Air Research Center. The contents do not necessarily reflect the views and policies of the sponsor, nor does the mention of trade names or commercial products constitute endorsement or recommendation for use.

8. Literature Cited

(1) Seinfeld, J. H.; Pandis, S. N. [1/4] Chapters 1-7. In *Atmospheric Chemistry and Physics: From Air Pollution to Climate Change (2nd Edition)*; Wiley-Interscience, 2006; pp 1–313.

(2) Lambe, A. T.; Zhang, J.; Sage, A. M.; Donahue, N. M. Controlled OH Radical Production via Ozone-Alkene Reactions for Use in Aerosol Aging Studies. **2007**, *41* (7), 2357–2363.

(3) Atkinson, R.; Aschmann, S. M. Oh Radical Production from the Gas-Phase Reactions of O-3 with a Series of Alkenes under Atmospheric Conditions. *Environ. Sci. Technol.* **1993**, *27* (7), 1357–1363.

(4) Rickard, A.; Young, J. DM23BU2ENE http://mcm.leeds.ac.uk/MCM/browse.htt?species=DM23BU2ENE.

(5) Yaws, C. L.; Gomes, J. A. *Transport Properties of Chemicals and Hydrocarbons*; 2009; Vol. 400.

(6) Leusink, J. How is Ozone Made? http://www.ozonesolutions.com/journal/tag/how-corona-discharge-makes-ozone/.

(7) 2,3-Dimethyl-2-butene (CAS 563-79-1) http://www.chemicalbook.com/ProductMSDSDetailCB8429788_EN.htm.

(8) Rickard, A.; Young, J. Toluene http://mcm.leeds.ac.uk/MCM/browse.htt?species=TOLUENE.

(9) Stedman, D. H.; Niki, H. Ozonolysis Rates of Some Atmospheric Gases. *Environ. Lett.* No. December 2013, 37–41.

(10) Klein, T.; Barnes, I.; Becker, K. H.; Fink, E. H.; Zabel, F. Pressure Dependence of the Rate Constants for the Reactions of Ethylene and Propene with OH Radicals at 295 K. **1984**, 5020–5025.